Sound transmission loss of rectangular and slit-shaped apertures: Experimental results and correlation with a modal model

Nicolas Trompette and Jean-Louis Barbry
Laboratoire Réduction du Bruit au Travail, Institut National de Recherche et de Sécurité (INRS), Avenue de Bourgogne, 54500 Vandoeuvre, France

Franck Sgard and Hugues Nelisse
Institut de Recherche Robert-Sauvé en Santé et Sécurité au Travail (IRSST), 505 Boulevard de Maisonneuve Ouest, Montréal, Québec H3A 3C2, Canada

(Received 28 May 2008; revised 10 September 2008; accepted 29 September 2008)

Among noise control techniques, enclosures are widely used. It is known that enclosure acoustic efficiency is strongly influenced by the presence of openings or leaks. Modeling of diffuse field sound transmission loss (TL) of apertures and slits is therefore critical when the enclosure acoustic performance characteristics need to be predicted with confidence either for design or for modifying existing enclosures. Recently, a general model for diffuse field sound TL of rectangular and circular apertures has been developed and validated with respect to existing analytical or numerical models. This paper presents an experimental validation of this new model. The aim was to develop a simple, reliable tool for predicting enclosure insertion loss using statistical energy analysis. Twelve out of the 15 test configurations were found to be reliable and were compared with theoretical models, which in fact correlate closely (without adjustment) with the experimental work.
 [DOI: 10.1121/1.3003084]

PACS number(s): 43.20.El, 43.55.Ti, 43.55.Fw, 43.55.Rg [KA] Pages: 31–41

I. INTRODUCTION

Among noise control techniques, enclosures are widely used. An enclosure must be absolutely airtight to ensure maximum acoustic efficiency. Even a small aperture (opening or leak) will significantly affect the acoustic efficiency of an enclosure.[1] Miller and Montone[2] revealed the effect of apertures on enclosure acoustic efficiency and their results are illustrated in the well-known graph (Fig. 1). Enclosure openings are usually designed for material flow, while leaks (slits or holes) result from poor assembly or engineering choices, such as using sliding gates. When the opening size is smaller than the acoustic wavelength, it is typically referred to as a leak; the term "opening" is generally used for larger opening sizes. Apertures must be prevented, minimized, or lined with sound absorption systems (sound traps and silencers) to ensure a good enclosure acoustic performance. In practice, however, opening influence and leak prevention are often overlooked. Quantification of opening and leak impact would be helpful when existing enclosure efficiency is insufficient and requires appropriate modification. For this reason, modeling of diffuse field sound transmission loss (TL) of apertures (openings, slits, and holes) can be considered a key process for correctly predicting enclosure acoustic performance at design stage and for assisting noise prevention specialists in performing appropriate design modifications to existing enclosures. This work forms part of a research project aimed at developing simple, efficient design tools for machinery enclosures based on statistical energy analysis (SEA). System responses are often analyzed in third-octave-bands, when applying SEA, whose parameters include nonresonant coupling loss factors based on evaluating sound TL between two subsystems. Therefore, the focus here is made on measuring and calculating third-octave-band sound TLs. Sgard *et al.*[3] recently undertook a comprehensive review of existing models and proposed a general, efficient, and rigorous numerical method based on a modal approach for predicting diffuse field TL of apertures with rectangular and circular cross sections. These authors also provided numerical results for this indicator and its relationship with the normal incidence case for various geometrical configurations. They concluded that the conventional third-octave normal incidence TL could be substituted for the diffuse field TL if adjusted by a correction factor.

Only comparisons between existing models and numerical results were provided in the paper of Sgard *et al.*[3] The present paper is intended to complement the work of Sgard *et al.*[3] by performing new third-octave-band experimental validation tests for rectangular openings and slits and to compare experimental results with the model of Sgard *et al.*[3] and other analytical models. It should be noted that while circular apertures have been presented in Ref. 3, these are not considered here for conciseness, but their testing is indeed planned for the future. The model agrees closely with experimental data for rectangular openings; as the paper subsequently shows, it is expected to also compare well for circular openings. This paper firstly provides a review of the literature to reveal the lack of available experimental data concerning rectangular opening and slit models. Experimental setup and investigated configurations are described in a second part. Third-octave-band experimental results are then presented and compared with existing values. Theoretical results derived from the model of Sgard *et al.*[3] for openings

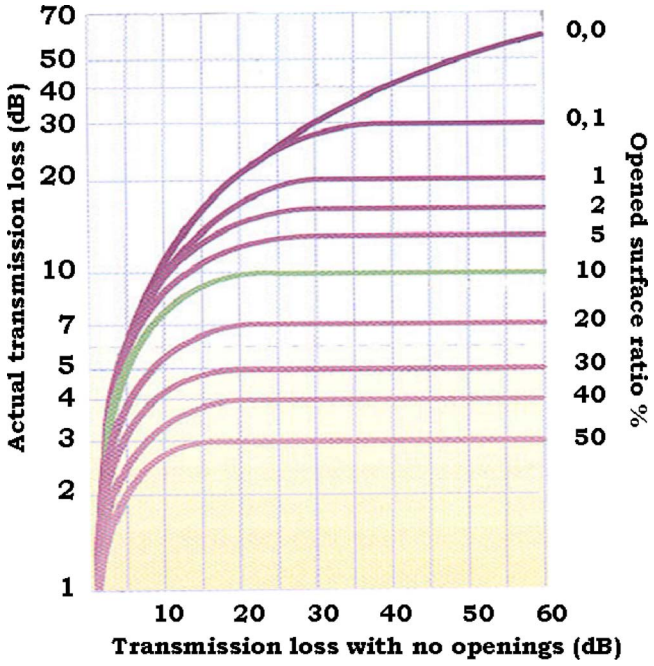

FIG. 1. (Color online) Maximum insertion loss of an enclosure as a function of the opened surface taken from Ref. 2.

and slits and from the model of Mechel[4] for slits, are subsequently compared with the experimental data. The main findings of this work are consolidated in our conclusion.

II. LITERATURE REVIEW

The relevant literature does not provide many diffuse field TL test results for apertures. Gomperts conducted a comprehensive study using two reverberant chambers interconnected by an 8 cm deep aperture.[5] Reproducibility, geometrical shape, and aperture location were all closely examined in this study. The aperture cross-sectional area varied fairly widely between 2 and 100 cm^2, and both rectangular and circular apertures were tested. Measurements were performed in third-octave bands from 630 Hz to 2 kHz. Measurement uncertainties were acceptable, except for the 1.6 kHz third-octave band, in which resonance of the first longitudinal mode occurs. These experiments were perfectly controlled and will be further investigated. Using the same test setup, Gomperts and Kihlman extended the previous survey to 2 m wide slits[6] with depths ranging from 1.5 to 100 mm and widths ranging from 0.5 to 8 mm. The results were less convincing than those of previous tests. Nevertheless, these 2 m wide slit results will be compared with measurements. Wilson and Soroka[7] also correlated their aperture model with experimental data. Several tests were conducted, but, unfortunately, only four are described in the authors' paper. The apertures studied were of circular cross section with 2 and 4 in. diameters and 3 and 12 in depths. The results of these tests are rather surprising: the TL frequency response appears correct, but the amplitudes are very high. This was noticed by the authors, who pointed out the small degree of damping in the recording system. These experiments must therefore be viewed with caution. Investigations were pursued by Sauter and Soroka,[8] applying exactly the same procedure to rectangular apertures. Twelve apertures, divided into four sets of three rectangular steel tubes, were tested. All tubes were 30 cm deep. The cross-sectional dimensions of each set were $\pi/4$, π, and 4π $in.^2$. The authors introduced an aspect ratio M (long side to short side ratio) and a geometrical parameter $\beta=h/(S^*\pi)^{1/2}$ (h=depth, S=cross-sectional area) for each set. Results were given for only five test configurations, corresponding to different combinations of M and β. Experimental data agreed closely with the models and can be used for further comparisons. More recently, Gibbs and Balilah[9] applied an impulse technique to measuring sound TL through circular holes. However, this technique involves meeting a number of strict conditions governing time signal generation and acquisition, and, more importantly, it is restricted to plane wave excitation. Furue[10] undertook an experimental study involving TL measurements of an aperture between a reverberant chamber and an anechoic room. However, this study focused on diffraction theory, so only high frequencies were considered. Oldham and Zhao[11] measured the circular aperture and slit TL of circular apertures and slits in a reverberant field source and compared their results with those of Wilson and Soroka's[7] and Gompert's[5] analytical models. These authors used the same experimental setup that used by Furue but took measurements in the receiving room with an intensity probe. Very small (4.5 and 10.2 mm diameters) circular apertures and 1 to 10 mm wide slits of different depths were tested. The narrow band results agree closely with the model predictions for the circular cross section case. Theoretical comparisons were less close for the slit case. The authors highlighted a discrepancy between theoretical and measured TLs at the fundamental resonance frequency for both circular cross section and slit cases. The deeper the aperture and the smaller the width or radius, the larger this discrepancy. This phenomenon was attributed to viscosity effects inside the aperture. It is interesting to note that the size of the tested circular apertures is unrealistic for enclosures. In addition, all results start at 1 kHz (small source room of 3.3 m^3) and are given in narrow bands, so they are not used in the present study. Finally, Chen[12] used a similar experimental setup for validating an infinitely long slit model similar to Mechel's model.[4] In this study, slit depth and length were 0.3 and 1.2 m, respectively (i.e., infinite width) for three widths: 7.8, 15, and 66 mm. Measurements were compared with both proposed normal incidence and diffuse field models for frequencies ranging from 100 to 1250 Hz. Differences between calculations and experiments were found to be smaller than 4 dB over the entire frequency range. According to Chen, the results seem reliable above 200 Hz. However, it is worth noting that the use of the normal incidence model leads to smaller discrepancies with respect to experimental data than the diffuse field theory. These results would therefore be questionable.

Table I consolidates papers available in the literature, which provide the reader with measurements that are usable for both openings and slits. Authors names, aperture shape, dimensions, and frequency range of interest are provided in different columns of this table. The table shows that there are a limited number of experimental data in the literature for

TABLE I. Summary of measurement data available in literature and usable.

Openings					
Author	Shape	Length or radius (cm)	Width (cm)	Depth (cm)	Frequency range (third-octave band)
Gomperts (Ref. 5)	Circular	0.2–100	⋯	11	630 Hz–2 kHz
	Rectangular	0.2–100	0.2–100	11	630 Hz–2 kHz
Wilson and Soroka (Ref. 7)	Circular	2.5/5	⋯	7.5/30	200 Hz–10 kHz
Sauter and Soroka (Ref. 8)	Rectangular β=6, M=2,4,8	3.2/4.5/6.4	25.6/18/12.8	30.48	200 Hz–6.3 kHz
	Rectangular β=6,12,24, M=8	3.2/1.6/0.8	25.6/12.8/6.4	30.48	200 Hz–6.3 kHz
Oldham and Zhao (Ref. 11)	Circular	0.45/1.02/2.04/3.98	⋯	3.6/7.26/14.4	~1 kHz–12 kHz

Slits					
Author	Shape	Length (m)	Width (mm)	Depth (cm)	Frequency range (third-octave band)
Gomperts and Kihlman (Ref. 6)	Rectangular	2	0.5/1/2/4	1.5/20/50/100	100 Hz–8 kHz
	Rectangular	0.2/0.5/1/2	4.5	50	100 Hz–8 kHz
Chen (Ref. 12)	Rectangular	1.2	0.78/1.5/6.6	30	100 Hz–5 kHz
Oldham and Zhao (Ref. 11)	Rectangular	Not specified	1/1.5/3/6	5.08/7.62/15.24	~1 kHz–12 kHz

validating aperture and slit models. New experiments therefore appeared necessary for validating the model proposed in Ref. 3. Some of these validation tests are similar to those contained in the literature. Apertures sizes were set according to dimensions tested by Sauter and Soroka.[8] Aperture depth was kept the same (30 cm). Two out of six configurations are effectively identical. Slits are identical to those used by Gomperts and Kihlman,[6] except for the 1 and 4 mm widths, which have not been tested. The dual purpose of this paper is, in fact, to reproduce data found in the literature and increase the number of available test results.

III. EXPERIMENTAL PROCEDURE

The purpose of the measurements was to obtain the diffuse field sound TL of openings and slits. Apertures were therefore located between an emission chamber and a receiving chamber.

The emission chamber was a 8 m^3 reverberant room, which was mounted on isolators to prevent flanking transmissions. The emission chamber was separated from the receiving chamber by a wall, part of which was concrete and part of which was steel plate (see the wall in Fig. 2). The two chambers were interconnected by a 0.41×0.55 m^2 aperture located in the center of the steel plate wall section. The diffuse sound field was produced by four noise sources, i.e. three Omni–Power sound sources and a compression chamber loudspeaker. Sound source generators were all uncorrelated, and the resulting noise spectrum was equalized, so that the acoustic energy was equally distributed in the third-octave bands. Sound pressure was measured at four different points in the chamber, which allowed its uniform spatial distribution to be verified (see Fig. 3). Incident acoustic energy was deduced from the sound pressure level averaged for the four microphone positions. The number of microphones was chosen based on Ref. 7.

The receiving room was an anechoic chamber. Transmitted acoustic energy was deduced from sound intensity point mapping measurements (see Fig. 2). Meshing was dependent on the size of the test aperture. Intensity measurement point spacing was coarser for large apertures and finer for slits. For large openings, 100 uniformly distributed measurement points were used with a 10 cm spacing in both aperture length and width directions. Measurement points were distributed on two different grids for the smallest slits. A fine grid for measurement points closest to the slit center was

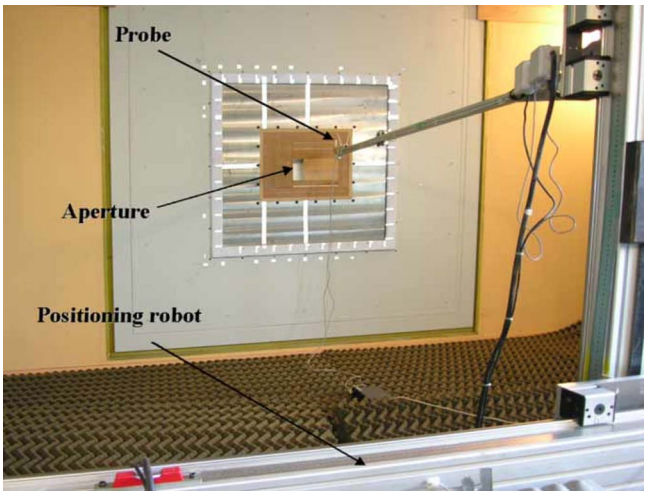

FIG. 2. (Color online) Receiving chamber with the intensity scanning device.

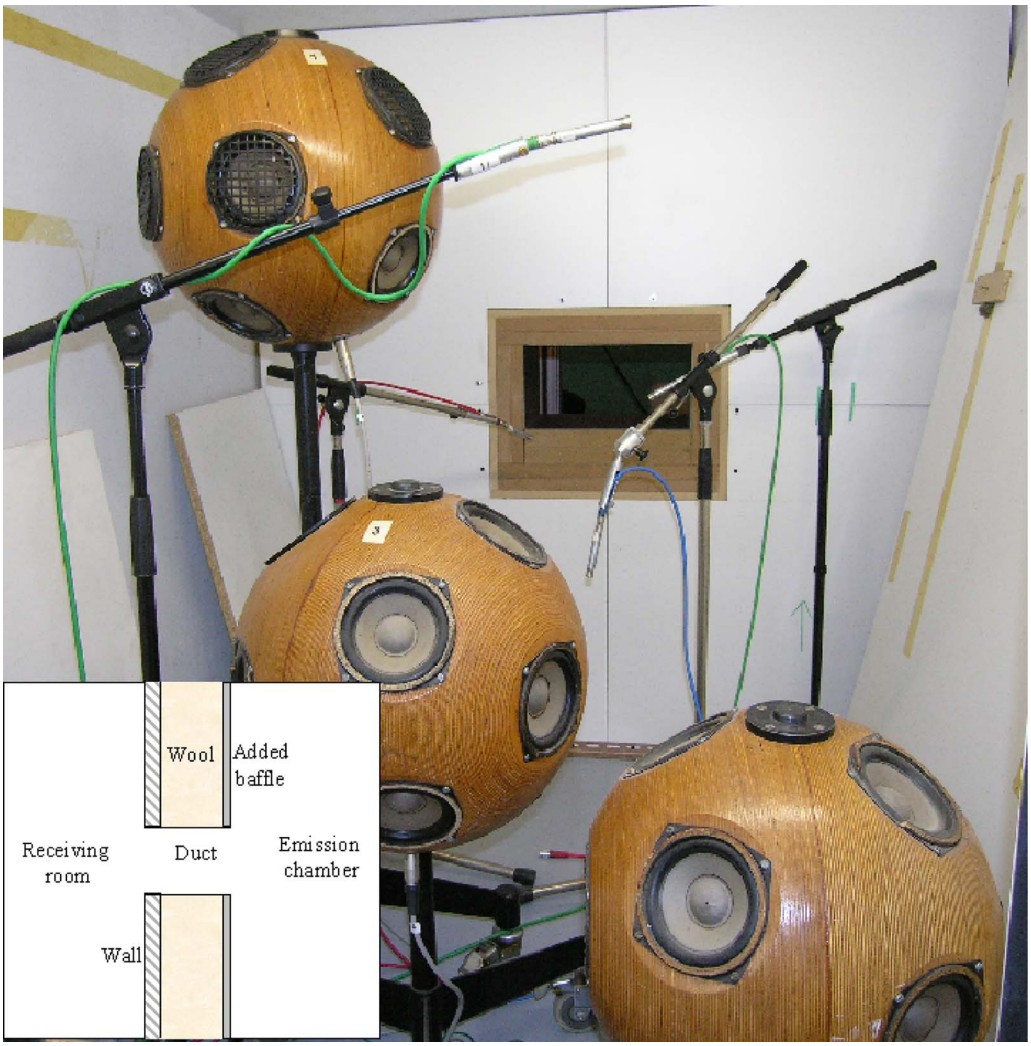

FIG. 3. (Color online) Emission chamber with three omni power sound sources and four microphone positions.

complemented by a coarser grid for more distant measurement points. 70 measurement points were used in the finer grids with a 4 cm spacing in the aperture length direction and a 2 cm spacing in the aperture width direction. 58 measurement points were used for the coarsest grid with a 8 cm spacing in the aperture length direction and a 6 cm spacing in the aperture width direction. At least 100 measurement points were used irrespective of the configuration. In the reverberant room, the sound power incident on the aperture (or the slit) W_i is deduced from the average pressure using the relation

$$W_i = \frac{\langle p^2 \rangle}{4\rho c} S, \tag{1}$$

where

- $\langle p^2 \rangle$ is the mean square pressure averaged for the four microphone positions
- ρ and c are the air density and sound speed, respectively
- S is the aperture cross-sectional area

In the anechoic chamber, the sound power W_t transmitted by the aperture was calculated from the sound intensity field using the relation

$$W_t = \sum_{j=1}^{N} I_j \Delta S_j, \tag{2}$$

where

- I_j is the sound intensity at point j
- ΔS_j is the surface area element around point j
- N is the number of the measurement grid points

The TL of the aperture is defined as

$$\mathrm{TL} = 10 \log \frac{W_i}{W_t}. \tag{3}$$

Measurements are valid as long as the acoustic field can be considered diffuse and uniform in the emission chamber. Several investigations have been performed to evaluate the frequency validity range. The Schröeder frequency[13] was calculated from the measured reverberation time and was found to be 705 Hz. Subsequently, an array of eight microphones spaced at 160 mm was used to check acoustic field uniformity (by comparing third-octave-band levels). The field was found to be uniform above 630 Hz. Differences in levels between microphones were smaller than ± 2 dB in the

TABLE II. Geometrical characteristics of test apertures.

Aspect ratio M b/a	Geometrical parameter β $\beta=h/(S^*\pi)^{1/2}$	Width a (mm)	Height b (mm)	Depth h (cm)	Third octaves
2	2	190	380	30	500 Hz–6.3 kHz
1	2	270	270	30	500 Hz–6.3 kHz
2	6	60	120	30	500 Hz–6.3 kHz
1	6	90	90	30	500 Hz–6.3 kHz
8	6	30	240	30	500 Hz–6.3 kHz
1	12	45	45	30	500 Hz–6.3 kHz

250–630 Hz range. The coherence between a microphone positioned near the aperture and the microphone array was also examined. The field, in fact, became incoherent between 250 and 315 Hz, depending on the microphone considered. These results indicate that measurements cannot be representative of diffuse field conditions below 250 Hz. However, these conditions are found to be acceptable in the frequency range (250–630 Hz) and good above 630 Hz.

The receiving room volume was 54 m^3. It was lined with 20 cm thick mineral wool. Its absorption reaches 1 at 400 Hz, and it can therefore be considered anechoic above this frequency. In addition, measurements were taken using the intensity method. Standard ISO 9614-2 states that the intensity method can be extended down to 100 Hz with a 12 mm microphone spacing.

The six openings were formed by 30 cm deep rectangular steel ducts. Table II shows the different cross-sectional areas of these ducts. The apertures needed to be baffled to comply with the model hypothesis. The duct depth exceeded the thickness of the separating wall between the emission and the receiving rooms, so an additional baffle was added inside the reverberant chamber with the aperture located at its center (Fig. 3). The cavity between the baffle and the chamber separating wall was filled with mineral wool to eliminate the cavity mode effects. The steel duct was positioned inside a larger rectangular wooden frame (0.51 $\times$0.4 m^2) to facilitate aperture installation. The gap between the duct and the wooden frame was made up with additional pieces of wood, which could be easily adjusted to prevent leaks (see Fig. 4).

Slits were built using two steel plates (1.5 and 20 mm thick) or wooden (50 mm thick) panels inserted into the primary aperture and separated by spacers. This arrangement ensured a slit depth equal to the plate thickness and a slit width equal to the spacer width (Fig. 5). The plates were 50 cm long, and the slits could therefore be considered infinite in the studied frequency range. This assembly had the advantage of a simple design. However, unlike the mounted aperture, leaks could occur at fixing points, and plate or panel TL could influence results. Special care was therefore taken to prevent leaks around fixing points, and additional tests were conducted to evaluate the contribution of the plate or panel to the acoustic power generated by the system. Table III shows the nine configurations, which were tested.

In addition, three transmitted sound power measurements were taken with the aperture or slit closed. In these configurations, the transmitted sound power was effectively inherent to the separating wall and the flanking transmission, and it represented the part of the sound not transmitted by the opening or slit. Measurements were used only when this transmitted sound power measurement was lower (at least 6 dB) than that transmitted by the opening or slit.

IV. EXPERIMENTAL RESULTS

The presentation of results is divided into two sections: the first focusing on openings and the second on slits.

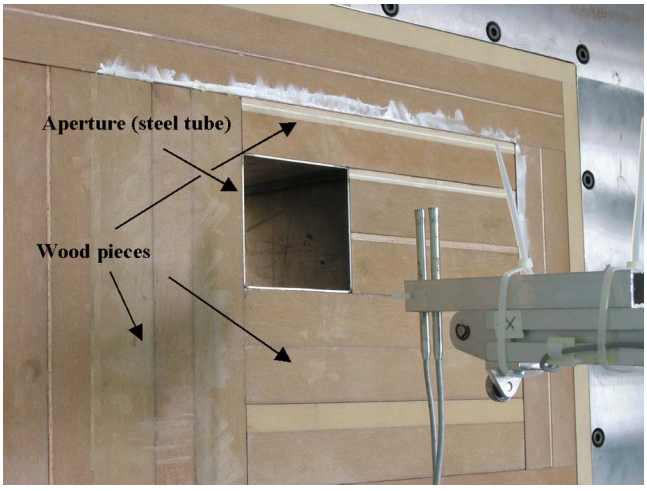

FIG. 4. (Color online) Aperture assembly, constituted of a steel tube and some pieces of wood filling a larger wood tunnel.

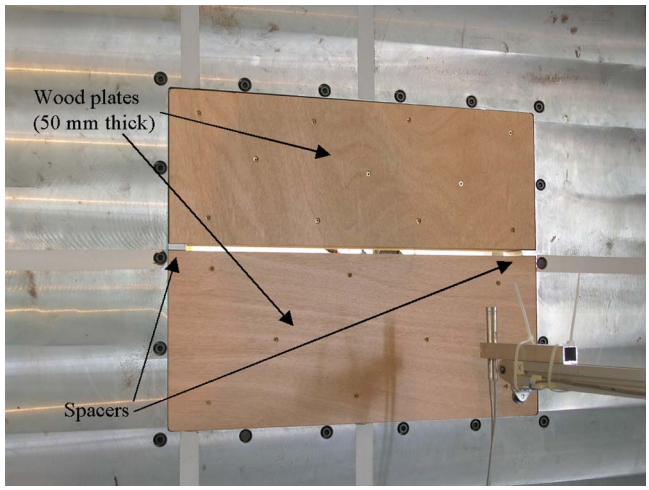

FIG. 5. (Color online) Leak made up by two plates separated by spacers.

TABLE III. Geometrical characteristics of test slits.

Length (mm)	Width (mm)	Depth (mm)	Third-octave central frequencies
500	0.5/2/8	1.5	500 Hz–6.3 kHz
500	0.5/2/8	20	500 Hz–6.3 kHz
500	0.5/2/8	50	500 Hz–6.3 kHz

A. Opening case

Literature-based data refer to rectangular apertures 18 and 30.48 cm deep.[5,8] One of the measurement aims was to compare experimental results with the literature. 30 cm deep openings (similar to experiments described in Ref. 8) only were studied because each opening depth change requires fabrication and assembly of a baffled transmission tunnel.

Reference 5 states that the cross-sectional shape has no practical consequences on sound transmission. Theoretically, this assumption is valid up to the aperture cutoff frequency. It was therefore interesting to test large apertures and to compare those with the same cross section but different shapes. The tested apertures thus have three different cross-sectional areas to (i) cover a wide range of aperture aspect ratios and dimensions, (ii) compare results for apertures of the same cross-sectional area, and (iii) compare results with those of Ref. 8.

Experimental results for the first two configurations in Table II ($M=2$, $\beta=2$) and ($M=1$, $\beta=2$), corresponding to the largest apertures, are shown in Fig. 6, and the corresponding TL values are listed in Table IV. Despite the small size of the emission chamber, the sound TL for these first two apertures exhibit a typical behavior above 250 Hz. Below the first longitudinal mode resonance, the TL is indeed positive and fairly large. It decreases rapidly at the mode resonance and becomes negative before finally tending to zero at high frequencies. The TL is zero above 800 Hz, as can be expected for the large aperture size. The differences between the two configurations do not exceed 2 dB, and the mean difference between the two configurations is 0.6 dB, which is insignificant.

Figure 6 also illustrates the experimental TL for the next three apertures in Table II, ($M=2$, $\beta=6$), ($M=1$, $\beta=6$), and ($M=8$, $\beta=6$). Experimental values are tabulated in Table IV. These apertures have the same cross-sectional area but different aspect ratios. The same conclusions apply. The TL maximum difference between the three configurations is 4 dB and is lower than 2 dB above 500 Hz. These aperture sizes are typical of those found in the industry. TL amplitude is high and can be negative, which underlines the importance of good aperture design.

The last aperture tested is the smallest. For conciseness, the results are also plotted in the top graph in Fig. 6 and tabulated in Table IV. This aperture is too small to be realistic, but this configuration will be the most relevant for comparing with the numerical models because the TL plot appears to have many dips and troughs. The reason for this is the aperture duct modal density, which is lower than for larger apertures.

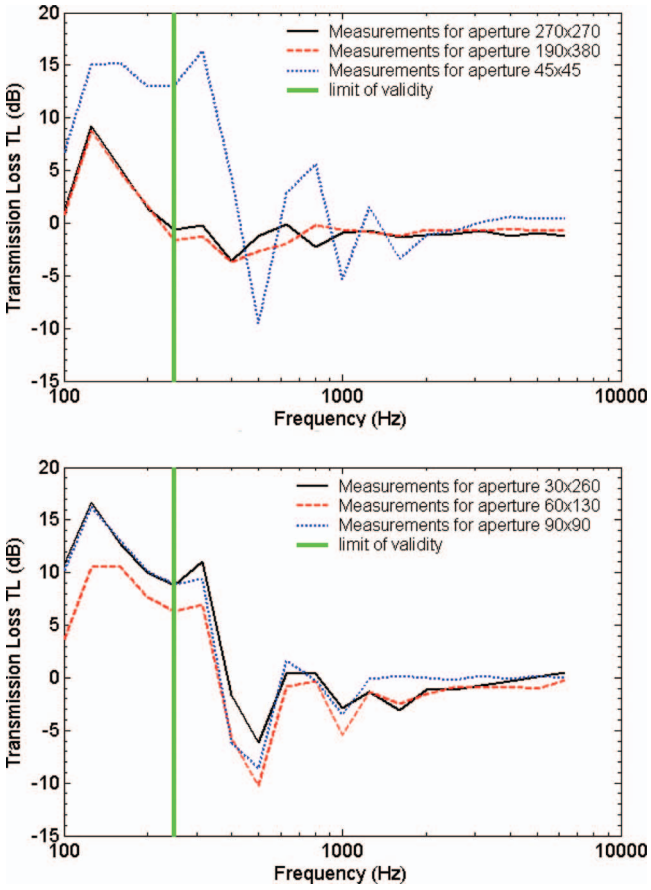

FIG. 6. TL of apertures—experimental results.

Intermediate size apertures (i.e., cross-sectional areas 30×260 and 60×130 mm^2) were also tested by Sauter and Soroka.[8] Figure 7 provides a comparison. It should be noted that there is an error in Ref. 8: the axis is, in fact, reversed in Fig. 5. Measurement correlation is very good, particularly if one considers the fact that the dimensions were not exactly the same and that the test setup was different.

B. Slit case

References 6, 11, and 12 contain some experimental data on slits. In this study, tests were only conducted on some of the configurations considered in Ref. 6. However, it is explained later that the data provided in Ref. 6 does not appear to be reliable.

Approximately half of the configurations tested by Gomperts and Kihlman[6] were retested (Table III). Figure 8 displays the results, which are also tabulated in Table V. It is important to emphasize that the transmitted acoustic power is very low, especially for the 50 mm deep slits. Flanking transmission and the transmission through the wall were both measured for these configurations. When the difference with respect to transmission through the slit was lower than 6 dB, an adjustment was made by subtracting the flanking transmission contribution to the radiated acoustic power from the overall radiated acoustic power. This is the case for the two 50 mm deep, 2 and 0.5 mm wide slits. Differences varied from 5 dB at 250 Hz to 15 dB at 6.3 kHz for the 2 mm wide slit and from 0.5 dB at 315 Hz to 6 dB at 6.3 kHz for the

TABLE IV. Experimental results for openings.

Aperture size	90×90	130×60	270×270	390×190	260×30	45×45
Frequency (Hz)	Transmission loss (dB)					
250	8.8	6.4	−0.6	−1.7	8.7	13.1
315	9.4	7.0	−0.2	−1.2	11.0	16.4
400	−6.1	−5.7	−3.6	−3.7	−1.6	4.4
500	−8.6	−10.2	−1.2	−2.6	−6.1	−9.6
630	1.6	−0.8	−0.1	−2.0	0.4	2.9
800	−0.2	−0.3	−2.2	−0.2	0.4	5.6
1000	−3.5	−5.4	−0.9	−0.6	−2.9	−5.3
1250	−0.1	−1.4	−0.8	−0.8	−1.3	1.5
1600	0.2	−2.5	−1.4	−1.2	−3.1	−3.4
2000	0.0	−1.5	−1.1	−0.6	−1.1	−1.1
2500	−0.2	−0.9	−1.0	−0.7	−1.2	−0.7
3150	0.2	−0.9	−0.7	−0.8	−0.7	0.1
4000	−0.1	−0.8	−1.2	−0.5	−0.3	0.6
5000	0.2	−1.1	−1.0	−0.8	0.1	0.4
6300	0.0	−0.2	−1.2	−0.7	0.5	0.4

0.5 mm wide slit. For these two slits, flanking transmissions prevailed below 250 and 315 Hz, respectively. The results for these two test configurations must therefore be accepted with caution. Comparisons between slits of the same depth show that the configuration differences agree with the width difference and the theoretical models (in particular, see Ref. 12).

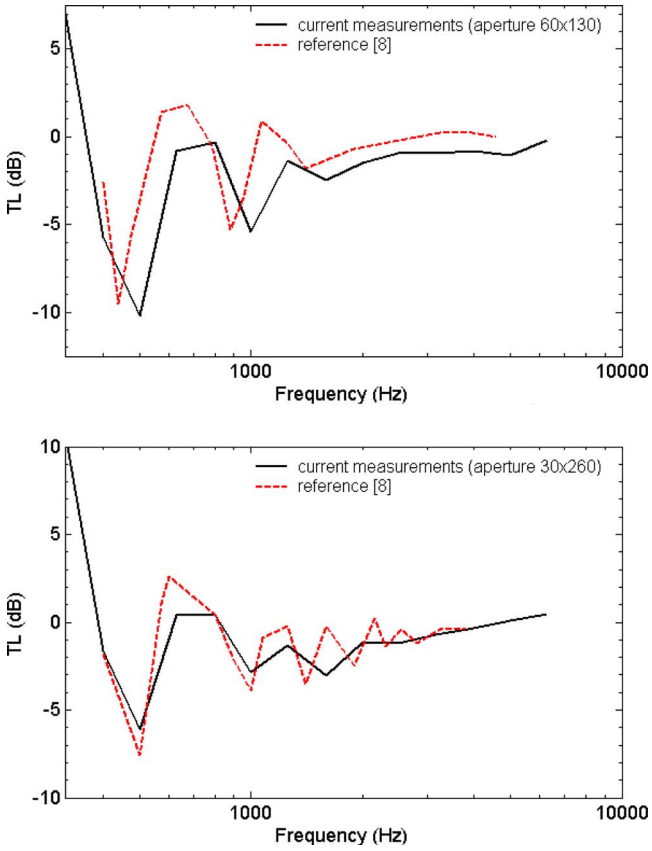

FIG. 7. (Color online) Comparison between the current measurements and data from Ref. 8 for rectangular apertures of dimensions $60\times130\times300$ mm^3 ($M=2$, $\beta=2$) (top) and $30\times260\times300$ mm^3 ($M=8$, $\beta=2$) (bottom).

This is particularly clear in the top graph in Fig. 8, which corresponds to the only configuration for which flanking transmission can be neglected. Based on Refs. 6 and 12,

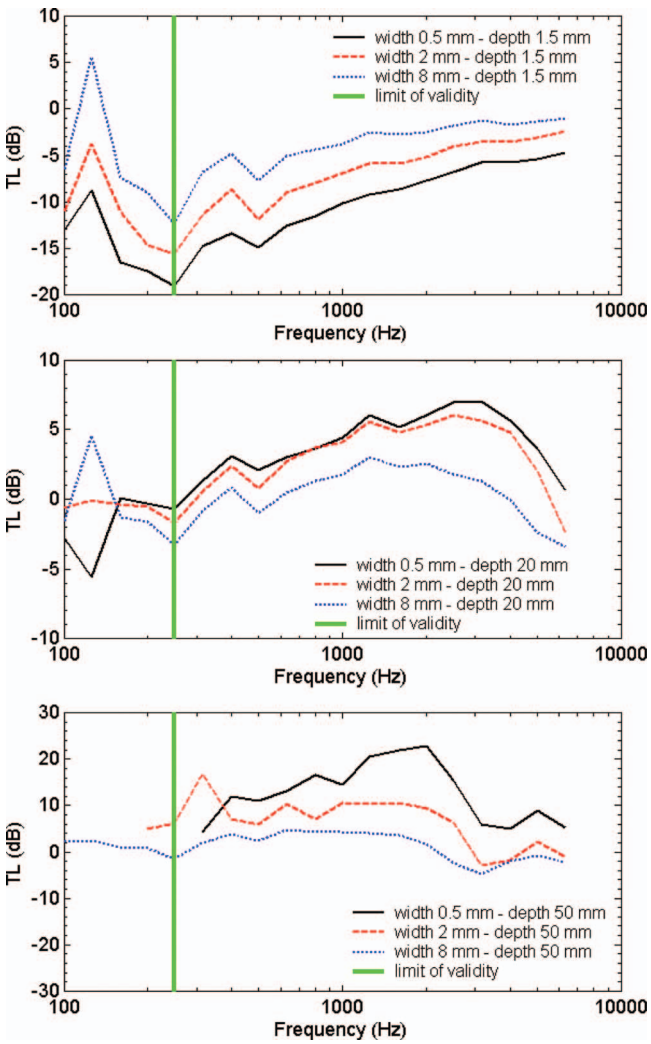

FIG. 8. TL of slits—experimental results.

TABLE V. Experimental results for slits.

Slit size	50×8 ×500 mm^3	50×2 ×500 mm^3	50×0.5 ×500 mm^3	20×8 ×500 mm^3	20×2 ×500 mm^3	20×0.5 ×500 mm^3	1.5×8 ×500 mm^3	1.5×2 ×500 mm^3	1.5×0.5 ×500 mm^3
Frequency (Hz)	Transmission loss (dB)								
250	−1.4	6.0	—	−3.3	−1.7	−0.7	−12.3	−15.6	−19.1
315	2.0	16.8	4.2	−0.8	0.5	1.4	−6.8	−11.5	−14.9
400	3.8	7.0	12.0	0.9	2.4	3.1	−4.9	−8.6	−13.4
500	2.4	5.9	10.9	−1.0	0.8	2.1	−7.7	−11.9	−15.0
630	4.7	10.4	13.8	0.4	2.7	3.0	−5.1	−9.0	−12.6
800	4.2	7.2	16.6	1.3	3.7	3.6	−4.4	−8.0	−11.5
1000	4.2	10.5	14.5	1.8	4.1	4.4	−3.8	−6.9	−10.2
1250	4.1	10.2	20.5	3.0	5.6	6.0	−2.5	−5.9	−9.3
1600	3.5	10.5	22.0	2.4	4.8	5.2	−2.8	−5.8	−8.6
2000	1.8	9.3	22.8	2.5	5.4	6.1	−2.5	−5.1	−7.7
2500	−2.5	6.4	15.5	1.8	6.1	7.0	−1.8	−4.1	−6.8
3150	−4.8	−2.8	5.9	1.3	5.7	7.0	−1.2	−3.6	−5.7
4000	−1.9	−1.6	4.9	−0.1	4.8	5.7	−1.6	−3.5	−5.8
5000	−0.9	2.2	8.9	−2.4	2.0	3.6	−1.3	−3.1	−5.4
6300	−2.3	−1.1	5.1	−3.4	−2.4	0.6	−1.0	−2.4	−4.7

the TL for this small depth (1.5 mm) should also show negative values and should behave smoothly as a function of frequency. This has been confirmed above 500 Hz, in accordance with the fact that the incident sound field can only be considered perfectly diffuse at 630 Hz. In the bottom graph in Fig. 8, the differences between 2 and 0.5 mm widths for a 500 mm deep slit are not as large as it would have expected, in view of the trend observed in the previous configuration (middle graph in Fig. 8) and in Ref. 12. This is probably due to the fact that the flanking transmission and the transmission through the separating wall were large for the 0.5 mm slit width configuration, particularly at third-octave center frequencies between 800 Hz and 1.25 kHz. For this depth, the TLs exhibit an erratic behavior due to both the adjustment referred to in the previous paragraph and the low transmitted power. It is important to highlight that this adjustment was not applied for the 8 mm slit width.

As mentioned above, slit dimensions were chosen to allow a comparison with the results published in Ref. 6. No such comparison is shown here because there were discrepancies up to 10 dB. It should be noted that this was already the case when Gomperts and Kihlman[6] failed to obtain satisfactory agreement between their experiments and the numerical models. The authors believe that there must be a problem in the experimental data presented in Ref. 6; this will be confirmed in the following section. While it is unfortunate that the results do not correlate, this does demonstrate how relevant it was to perform this new series of experiments

V. COMPARISONS WITH NUMERICAL MODELS

The model used for the comparison is the one proposed by Sgard *et al.* in Ref. 3, in which the authors reviewed all the main existing models for rectangular and circular apertures and developed a new model based on the modal approach. This model is briefly recalled in the following section. It is valid for both rectangular and circular openings and for leaks. Sgard *et al.*[3] showed that Mechel's analytical model for infinitely wide slits[14] compares perfectly well with the modal approach when the width of the slit is taken to be sufficiently large. The modal approach deals with finite width slits and becomes time consuming for slits that are very wide compared to the acoustic wavelength. Mechel's model can therefore be used as an alternative, thereby reducing computation time.

The model developed by Sgard *et al.*[3] is based on modeling the sound field within the aperture in terms of propagating and evanescent acoustic modes. Aperture radiation is considered by means of a modal radiation impedance matrix. The coupled problem is then solved in terms of modal contribution factors to obtain the transmission coefficient for any plane wave angle of incidence. The diffuse field (or field-incidence) transmission coefficient is finally obtained by integrating over all angles of incidence. Model details can be found in Ref. 3. To summarize, the sound transmission coefficient for a plane wave with an angle of incidence (θ, ϕ) is given by

$$\tau(\theta_i, \varphi_i) = -\frac{\rho_0}{k_0 \cos\theta_i \rho_f^* |\hat{A}_i|^2 S} \Re\left(\sum_M N_M \hat{k}_M^* \hat{C}_M \hat{D}_M^*\right), \quad (4)$$

where the summation is performed over the aperture lateral modes. Modal coefficients $\hat{C}_M$ and $\hat{D}_M$ are related to modal radiation impedances, the area of the aperture, and the impedance of the fluid within the aperture. Coefficients $\hat{k}_M$ and N_M are the modal wave number and the modal norm, respectively. Amongst the remaining factors, it is worth mentioning that $\hat{A}_i$ represents the amplitude of the incident plane wave.

The diffuse field (or field-incidence) TL of the aperture is therefore given by

$$\mathrm{TL} = -10 \log_{10}(\tau_d), \quad (5)$$

where

$$\tau_d = \frac{\int_0^{2\pi}\int_0^{\theta_{\lim}} \tau(\theta_i,\varphi_i)\sin\theta_i \cos\theta_i d\theta_i d\varphi_i}{\pi \sin^2\theta_{\lim}}. \quad (6)$$

The diffuse field TL is obtained by setting the angle $\theta_{\lim}$ to 90°, while the field-incidence TL is defined by setting $\theta_{\lim}$ to 78°. The integrals in Eq. (6) are performed numerically. The model results presented in the following sections use the field-incidence TL.

In the case of Mechel's model[4] for slits of width b and depth d, the transmission coefficient is relatively easy to obtain and is given by

$$\tau(\theta_i,\varphi_i) = \frac{Z_0}{\cos\theta_i}\Re[\hat{Z}_{R2}]p_g^2 \left| \frac{\hat{Z}_a}{\hat{Z}_a(\hat{Z}_{R1}+\hat{Z}_{R2})\cos(\hat{k}_a d) + j(\hat{Z}_a^2+\hat{Z}_{R1}\hat{Z}_{R2})\sin(\hat{k}_a d)} \right|^2, \quad (7)$$

where $Z_0=\rho_0 c_0$ is the characteristic impedance of the external fluid, $\hat{Z}_{Ri}=Z_0\hat{Z}_{\text{slit},m}$ is the radiation impedance at the front ($i=1$) and rear faces ($i=2$) of the aperture, $\hat{Z}_f$ is the characteristic impedance of the fluid within the aperture, $\hat{k}_f$ is the wave number within the aperture, $p_g=2\,\text{sinc}(k_y b)$, $\hat{Z}_a=\hat{Z}_f/\cos\theta_f$, $\hat{k}_a=\hat{k}_f\cos\theta_f$, $k_y=k_0\sin\theta_i\sin\varphi_i$, k_0 is the wave number in the fluid outside the aperture, $\cos\theta_f=\sqrt{1-(k_0\sin\theta_i\cos\phi_i/\hat{k}_f)^2}$, and

$$\hat{Z}_{\text{slit},m} = 2k_0 b\left[H_0^{(2)}(u) + \frac{\pi}{2}[H_1^{(2)}(u)S_0(u) - H_0^{(2)}(u)S_1(u)] - \frac{1}{u}H_1^{(2)}(u) + \frac{2j}{\pi u^2}\right], \quad (8)$$

with $u=2b\sqrt{k_0^2-k_x^2}$, $k_x=k_0\sin\theta_i\cos\varphi_i$, and $H_0^{(2)}(u)$ and $H_1^{(2)}(u)$ as the zeroth and first order Hankel functions of the second kind, respectively.

Note that for very small cross-sectional areas and large depths, viscosity effects in the aperture may become significant and should be included in the calculation, as pointed out in Ref. 11. These effects can be included for both rectangular and circular cross sections using a simple model such as the one developed by Pierce.[14] This is based on expressing $\hat{k}_f$ as

$$\hat{k}_f = \frac{\omega}{c_f} + (1-i)\alpha_{\text{walls}}, \quad (9)$$

where

$$\alpha_{\text{walls}} = 2^{-3/2}\sqrt{\frac{\omega\mu}{\rho_f c_f^2}}\left[1+\frac{\gamma-1}{\sqrt{\text{Pr}}}\right]\frac{L}{A}, \quad (10)$$

in which μ is the dynamic viscosity, Pr is Prandlt number, ρ_f and c_f are the density and the sound velocity in the fluid within the aperture, respectively, and L and A are, respectively, the perimeter and the aperture cross-sectional area.

Equation (9) is valid for frequencies satisfying the condition

$$\left(\frac{L}{A}\right)^2\frac{\mu}{8\rho_f} < \omega < \left[\frac{9}{32}\left(\frac{L}{A}\right)^2\frac{\rho_f c_f^4}{\mu}\right]^{1/3}.$$

A. Opening case

Figure 9 illustrates the experimental data and the modal-based results for cases featuring two rectangular apertures with dimensions of $45\times45\times300$ and $60\times130\times300$ mm^3. It is clear that the experimental data match closely the calculation-based results, even in the low frequency range in which the incident field cannot be considered diffuse. No adjustments were made, and dimensions are those given in the tables. Modes have been kept up to a 10 kHz truncation frequency. An excellent correlation between the experimental data and the calculations confirms that these results can con-

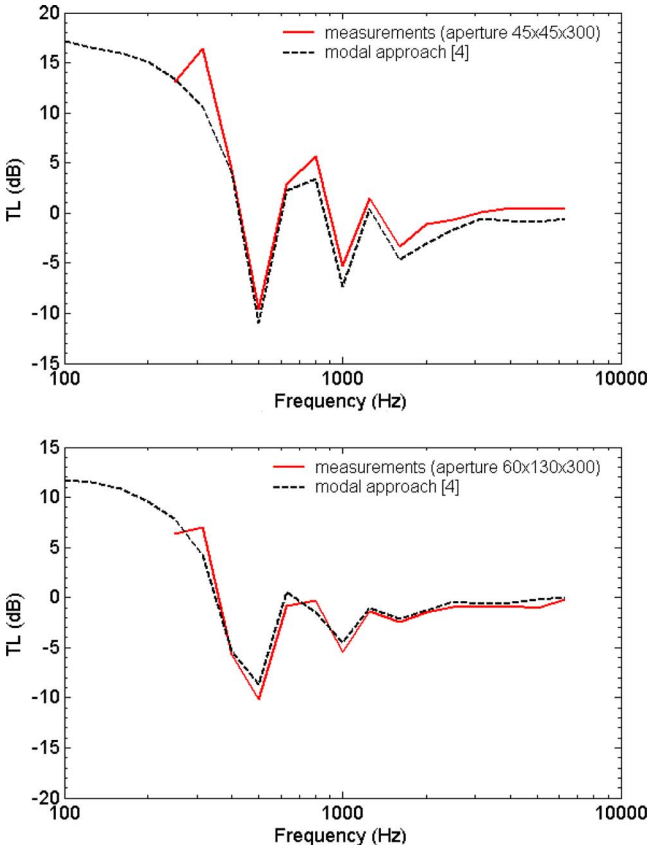

FIG. 9. (Color online) Comparison between experimental results and calculations for apertures of dimensions $45\times45\times300$ mm^3 (top figure) and $60\times130\times300$ mm^3 (bottom figure).

stitute a reliable set of experiments for the TL of baffled apertures exposed to a diffuse field. Correlation also underlines the accuracy of the model proposed in Ref. 3.

B. Slit case

The experimental results were compared with the two models (Mechel's[4] and modal approach[3]). It should be noted that viscous effects are taken into account in the calculations using Eq. (9). These effects are mainly important for slits with the smallest widths (0.5 and 2 mm) and the largest depth (50 mm) but are negligible otherwise.

For the smallest depth (1.5 mm), the experiments correlate fairly closely with the modal-based calculations above 500 Hz. Discrepancies can be attributed to nonuniformity of the incident field (see Sec. IV) below 630 Hz, although such discrepancies were not observed in larger openings (Fig. 9). In the slit case, the cutoff frequency is dictated by the slit length, which is very small. Oblique modes (which are numerous) can be excited in the frequency range of interest. The TL will therefore be more sensitive to nonuniformity of the incident acoustic field in this range. For openings, the cutoff frequency is thus higher at low frequencies, and it is primarily the plane wave mode that contributes to TL. However, the generalized force exerted on this mode is independent of the angle of incidence (see Ref. 3), and the TL is little influenced by nonuniformity of the incident acoustic field. Comparison leads to the same conclusions, except for the smallest width (not shown here for conciseness) for the medium slit depth (20 mm). As explained above, the difference between transmission through the slit and transmission through the wall in addition to flanking transmission is too low at this width, which is the reason for discrepancies. Measurements for this particular configuration cannot be used. The observation is the same for the largest slit depth (50 mm) and widths of 0.5 and 2 mm. The ratio between acoustic power transmitted through the slit and lateral transmissions is even worse. The discrepancies therefore accentuate and are unacceptable. Only the results for the 8 mm slit width are reliable for this 50 mm depth.

Correlation between experiments and modal-based calculations is acceptable above 500 Hz for the remaining six configurations. Figure 10 illustrates this for three of these configurations. This holds true irrespective of the considered model, i.e., Mechel's or modal approach. Correlation with Gomperts' model (not shown here for conciseness) is also acceptable. This tends to confirm that the series of tests described in Ref. 6 is unreliable.

VI. CONCLUSION

The purpose of this paper is to report new experimental diffuse field sound TL tests for rectangular openings and slits to validate the model developed in Ref. 3. This would provide additional reliable third-octave-band experimental data, which could be used in the framework of SEA.

This objective was fulfilled, although about half of the tests conducted on slits could not be used because of some uncertainties caused by flanking transmission paths. In the case of openings, experimental results were found to be reliable over almost all the frequency range of interest, namely, 250–5000 Hz. In the case of slits, only the results above the reverberant chamber cutoff transmission (630 Hz) are reliable.

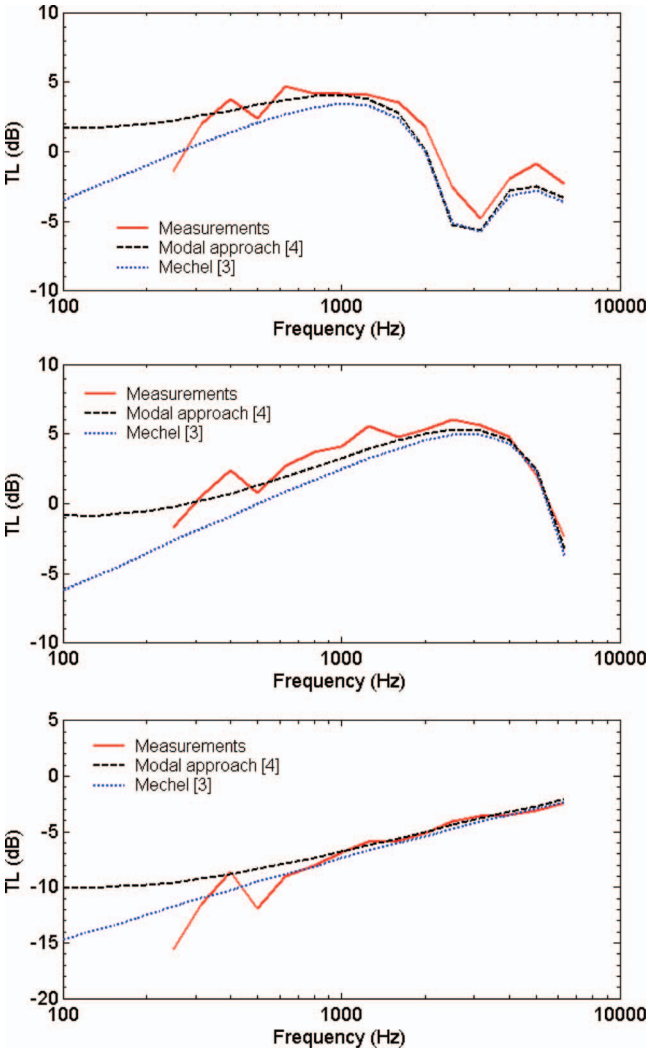

FIG. 10. Comparison between experimental results and calculations for slits of dimensions $500\times8\times5$ mm^3 (top figure) and $500\times2\times20$ mm^3 (middle figure), and $500\times2\times1.5$ mm^3 (bottom figure).

It was found that the modal approach correlates very closely with the experiments performed for all chosen configurations. This result, obtained with no adjustments, validates both the model and the tests. In addition, for sufficiently wide slits, Mechel's model[4] proves to be a faster alternative to the modal model, as observed in Ref. 3.

Future work will deal with modeling of apertures with acoustic linings, a configuration often encountered in industry, when the silencing equipment is fitted to apertures or when they comprise a simple hole in an acoustic panel.

ACKNOWLEDGMENTS

This research was undertaken within the framework of cooperation between IRSST and INRS. The research project scope involves developing accurate, easily applicable methods for modeling enclosures.

[1]H. Kuttruff, *Room Acoustics*, 2nd ed. (Applied Science, London, 1979).
[2]R. K. Miller and W. V. Montone, *Handbook of Acoustical Enclosures and Barriers* (Fairmont Press Inc., Atlanta, 1978).
[3]F. Sgard, H. Nelisse, and N. Atalla, "On the modelling of diffuse field sound transmission loss of finite thickness apertures," J. Acoust. Soc. Am. **122**, 302–313 (2007).
[4]F. P. Mechel, "The acoustic sealing of holes and slits in walls," J. Sound Vib. **111**, 297–336 (1986).
[5]M. C. Gomperts, "The sound insulation of circular and slit-shaped apertures," Acustica **14**, 10–16 (1964).
[6]M. C. Gomperts and T. Kihlman, "The sound transmission loss of circular and slit-shaped apertures in walls," Acustica **18**, 144–150 (1967).
[7]G. P. Wilson and W. W. Soroka, "Approximation to the diffraction of sound by a circular aperture in a rigid wall of finite thickness," J. Acoust. Soc. Am. **37**, 286–297 (1965).
[8]A. Sauter and W. W. Soroka, "Sound transmission through reverberant slots of finite depth between reverberant rooms," J. Acoust. Soc. Am. **47**, 5–11 (1970).
[9]B. M. Gibbs and Y. Balilah, "The measurement of sound transmission and directivity of holes by an impulse method," J. Sound Vib. **133**, 151–162 (1989).
[10]Y. Furue, "Sound propagation from the inside to the outside of a room through an aperture," Appl. Acoust. **31**, 133–146 (1990).
[11]D. J. Oldham and X. Zhao, "Measurement of the sound transmission loss of circular and slit-shaped apertures in rigid walls of infinite thickness by intensimetry," J. Sound Vib. **161**, 119–135 (1993).
[12]F.T. Chen, "Study of acoustic transmission through apertures in wall," Appl. Acoust. **46**, 131–151 (1995).
[13]J. M. Bruneau, "Acoustic of close space," *Fundamentals of Acoustic* (Hermes, Paris, 1998), Sec. 9.
[14]A. D. Pierce, *Acoustics: An Introduction to Its Physical Principles and Applications* (Acoustical Society of America, Woodbury, 1981), pp. 531–534.